Thermal Stability and Resistance to Biodegradation of Humic Acid Adsorbed on Clay Minerals

Igor Danilin , Inna Tolpeshta * , Yulia Izosimova , Lev Pozdnyakov , Olga Salimgareeva , Andrey Stepanov

Posted Date: 28 August 2023

doi: 10.20944/preprints202308.1813.v1

Keywords: clay minerals; sorption; humic acid; thermal stability; amphiphilicity; biodegradation

Article

Thermal Stability and Resistance to Biodegradation of Humic Acid Adsorbed on Clay Minerals

I.V. Danilin, I.I. Tolpeshta *, Yu. G. Izosimova, L.A. Pozdnyakov, A.A. Stepanov and O.A. Salimgareeva

Lomonosov Moscow State University
* Correspondence: itolp@soil.msu.ru

Abstract: This work studied sorption regularities and assessed thermal stability and resistance to microbial degradation of humic acid as a result of 3 sorption cycles on bentonite clay, kaolinite, and muscovite using TGA/DSC, XRD, hydrophobic chromatography, light and electron microscopy, etc. The experiment revealed that kaolinite sorbed more humic acids (HAs) in terms of unit surface area (1.03×10^{-3} C, g/m^2) compared to bentonite (0.35×10^{-3} C, g/m 10^{-3} g/m^2). Sorption at pH 4.5 was accompanied by HA fractionation in amphiphilicity and chemical composition. HA was sorbed mainly due to hydrophobic components on the surface of all sorbents. HA was not intercalated into the interlayer spaces of montmorillonite during sorption. Sorption due to hydrophilic interactions was mostly performed on muscovite and bentonite than on kaolinite. Sorption was followed by a change in the chemical composition of HA and decreased C/N compared to free HA, indicating selective sorption of nitrogen-containing compounds which is most characteristic of muscovite. Only a relatively thermolabile HA fraction was adsorbed on all minerals while its thermal stability increased compared to that before the experiment. Thermal stability and ratio of the Exo2/Exo1 peak areas on the DSC curves of sorbed HA increased with each subsequent sorption cycle. Thermal stability and resistance to microbial oxidation of sorbed HA showed the following relationship: the higher the thermal stability, the less available is sorbed HA for utilization by microorganisms.

Keywords: clay minerals; sorption; humic acid; thermal stability; amphiphilicity; biodegradation

1. Introduction

Stabilization of organic matter is one of the main factors ensuring the ecological functions of soil, and is the most important component of the global carbon cycle. One of the reasons for increasing the resistance of soil organic matter (SOM) to chemical oxidation and microbial degradation is its fixation on the mineral soil matrix [1,2]. The main mechanisms of SOM sorption on minerals include ligand exchange, formation of bridge bonds through polyvalent cations, hydrophobic and van der Waals interactions. These mechanisms occur in soil simultaneously, and predominance of one or another mechanism is determined by the properties of sorbent minerals, soil solution (pH, ionic strength) and organic matter dissolved in it [3–6].

SOM sorption on clay minerals increases with decreasing pH and increasing ionic strength [4,7–9], as well as in presence of iron cations [9,10], aluminum [11], calcium [12,13], and copper [14].

Numerous studies show that interaction of organic matter (OM) with the mineral soil matrix leads to increased thermal stability of organic matter [15–21]. Thermal analysis allows us to estimate the energy barrier of OM destruction or the stored energy released during microbiological destruction of OM [22–24]. Barré et al. established that burning more thermally stable soil organic matter releases less energy than burning thermolabile OM, and soil microorganisms prefer to oxidize high-energy OM, leaving material with a low energy store [17]. Peltre et al. revealed a negative relationship between the resistance of organic matter sorbed on the surface of minerals to microbial action and its thermal stability [24].

 doi:10.20944/preprints202308.1813.v1

However, the relationship between resistance to microbial degradation and thermal stability is not always absolute [22–25]. Zhang et al. showed that low molecular weight SOM fractions can be strongly retained in micropores [10]. In this case, it becomes more difficult for microbes to decompose organic matter and its resistance to microbial decomposition increases significantly [3,16,26], while thermal stability remains unchanged. In addition, the literature provides the results of sorption experiments with sorbates and sorbents of different compositions and under different sorption conditions, which makes it difficult to compare and outline general sorption regularities, thermal stability, and resistance to microbial oxidation of the sorbed organic matter.

In nature, organic matter sorption occurs both on the surfaces of minerals and on new sorption centers made by the sorbed organic matter. Considering the zonal model of organomineral interactions [16], the sorbed organic matter at different distances from the surface is likely to have different thermal characteristics, different chemical composition, and different resistance to microbial oxidation.

The purpose of this study was to assess resistance to thermal effects and microbial oxidation of humic acid fixed on the surface of kaolinite, muscovite and bentonite during three sorption cycles.

2. Materials and Methods

Sorbents. Sorption experiments were carried out using bentonite clay, kaolinite, and muscovite. Bentonite clay was selected from the Sarigyuh deposit (the Republic of Armenia). A detailed description of bentonite is given in the work by Chechetko et al [27]. Kaolinite was produced at the Prosyanovsk deposit (Ukraine). Muscovite was produced by JSC "GEOKOM" and is sold under the commercial name "FRAMIKA".

Sorbate. A commercial product of potassiumhumate ("POWHUMUS" (Humintech GmbH, Dusseldorf Hansaalee 201, D-89079) isolated from leonardite was used as a sorbate. According to Semenov's data, the humic product has the following elemental composition (wt %): carbon - 51.5; hydrogen - 4.2, nitrogen - 1.5, oxygen - 42.8. The ash content is 26.8% and the degree of oxidation is 0.3. The number average molecular weight is 4 kDa, and the weight average molecular weight is 16 kDa. The product contains 496 mmol(eq)/100 functional groups, including 260 carboxyl and 236 phenolic groups with pKa 4.5, 6.5, and 9.5 [28].

Sorption procedure of humic acid (HA) on minerals. Bentonite clay, kaolinite and muscovite were treated with 10% HCl to remove calcium and magnesium carbonates. The kaolinite treated with hydrochloric acid was washed from excess acid, dried, ground in an agate mortar, and used in that form for experiments. The bentonite and muscovite treated with hydrochloric acid were washed to remove excess reagent, and a fraction <1 μm was isolated from them by the sedimentation method (precipitant was a 1 mol/L $CaCl_2$ solution). The resulting clay fraction was washed from excess chloride ion by dialysis, dried and ground in an agate mortar, and used for subsequent experiments.

A sample of the HA product was dissolved in 5 mmol/L acetate buffer (pH = 4.5). The concentration of the working solution of HA was 100 mg/l. The resulting solution was poured into weighed samples of minerals at a ratio of solid phase: liquid equal to 1:1000 into flasks with a volume of 250 ml and shaken on a shaker for 5 h at 150 rpm. The resulting suspension was centrifuged at 489g (OS-6MTs centrifuge, Kyrgyzstan) within 15 minutes. The resulting precipitate was quantitatively transferred into porcelain cups and dried at 40°C. The dried sample was again ground in an agate mortar and the sorption–drying procedure was repeated two more times. An aliquot of the supernatant was centrifuged at 16639g (Eppendorf 5804 centrifuge, rotor FA-45-6-30, Germany) for 30 min and stored to determine amphiphilicity.

Assessing stability of the original and mineral-sorbed HA to microbial action. Samples of minerals after three sorption cycles were incubated in glass vials in the ratio of solid:liquid phase = 1:0.8 (1.5 g of the mineral : 1.2 ml of distilled H_2O at 25°C in the dark in several stages: the first stage of incubation took 90 hours, the following 4 stages - 70 hours each. To determine basal respiration at the end of each incubation stage, the gas phase was taken with a syringe and the concentration of carbon dioxide in it was determined by gas chromatography on a Crystal 5000.2 chromatograph (Khromatek, Russia).

 doi:10.20944/preprints202308.1813.v1

Basal respiration of the humic acid solution was measured with an OxiTop-C biological oxygen demand (BOD) manometric system in the presence of a nitrification inhibitor (allylthiourea) during the same time intervals as with minerals.

Assessing thermal stability of the original and mineral-sorbed HA. Thermal analysis was performed on a TGA/DSC 3+ synchronous thermal analyzer (Mettler Toledo, Switzerland) equipped with an o-DTA sensor that did not require a reference sample. Calibration of the device was carried out according to the temperature and melting enthalpy of certified materials - indium, zinc, aluminum and gold. The samples were taken in a synthetic air atmosphere (composition: 80% N_2, 20% O_2) with a gas flow rate of 60 ml/min in aluminum oxide crucibles with a volume of 70 μl, the heating rate was 10 °C/min. Before analysis, the samples were kept for several days in a desiccator over a saturated solution of calcium nitrate to maintain a constant relative humidity of 55%. The sample weight varied depending on organic matter content and was approximately 50 mg for pure minerals, 30 mg for minerals treated with HA, and 15 mg for the HA product. All measurements were carried out in duplicate. The experimental curves were processed using STARe Evaluation Software (v. 16.40).

To calculate the area of exothermic peaks, the Fityk program (v. 1.3.1) was used; the baseline was drawn by a spline function with extreme points in the regions of 150–200°C and 550–800°C [29]. Identification of weight loss areas was carried out visually by comparing the weight loss curves with the peaks of the weight loss rate according to the DTG curves.

Amphiphilicity of HA. Amphiphilicity of HA was studied by hydrophobic chromatography on a BIOLOGIC LP chromatographic system (BIO-RAD, USA). Modified agarose Octil-Sepharose CL 4B (Pharmacia) was used as a working matrix. The following conditions were chosen for humic substance (HS) separation: column - 1.84 X 6.5 cm (BIO-RAD); buffer - 0.05 M Tris-HCI pH 7.2; sensitivity - 0.2-0.4% T; elution rate - 5 ml/h; detection was carried out at 206 nm. Linear concentration gradients of ammonium sulfate ranged from 2.0 to 0 M, detergent - from 0 to 0.3% SDS-Na. The proportion of hydrophobic and hydrophilic components was calculated from the peak areas in the chromatograms.

Elemental composition of HA. Elemental analysis was performed on a Vario EL III CHNS analyzer (Elementar, Germany) in triplicate.

Specific surface area. The surface area was determined on a Quadrasorb SI/Kr analyzer (Quantachrome Instruments, USA). Adsorption was carried out at a temperature of 77.35 K; nitrogen with a purity of 99.999% was used as the adsorbate. Helium of 99.9999% purity was used to calibrate the volume of the measuring cells. Calculation was carried out according to the BET isotherm in the P/P_0 range from 0.05 to 0.30.

Mineral composition of sorbents. The mineral composition of sorbents was determined by X-ray diffractometry on a MiniFlex 600 diffractometer (Rigaku, Japan) in the following mode: CuKα radiation, voltage and current in the X-ray tube 30 kV and 15 mA, detector –D/teX.

Microscopy. Studies at the micro- and submicrolevels were performed using a Soptop CX40P specialized direct polarizing optical microscope (Sunny Optical Technology, China) and a JEOL JSM-6060A scanning electron microscope (JEOL, Japan).

Data visualization. The visualization of the experimental data was conducted utilizing the R package ggplot2 [30].

3. Results

Mineral composition of sorbents. The kaolinite sample contained small amounts of mica with d (001) 1.01 nm (Figure 1A). The diffraction pattern of muscovite showed weak peaks from kaolinite (0.72 nm), quartz (0.426 nm), and feldspars (0.322 nm) (Figure 1B). The silty fraction of bentonite clay consisted mainly of montmorillonite. Interplanar spacing of montmorrilonite in the Ca form was 1.49 nm and increased to 1.72 nm after saturation with ethylene glycol (Figure 1B).

Preprints (www.preprints.org) | NOT PEER-REVIEWED | Posted: 28 August 2023 doi:10.20944/preprints202308.1813.v1

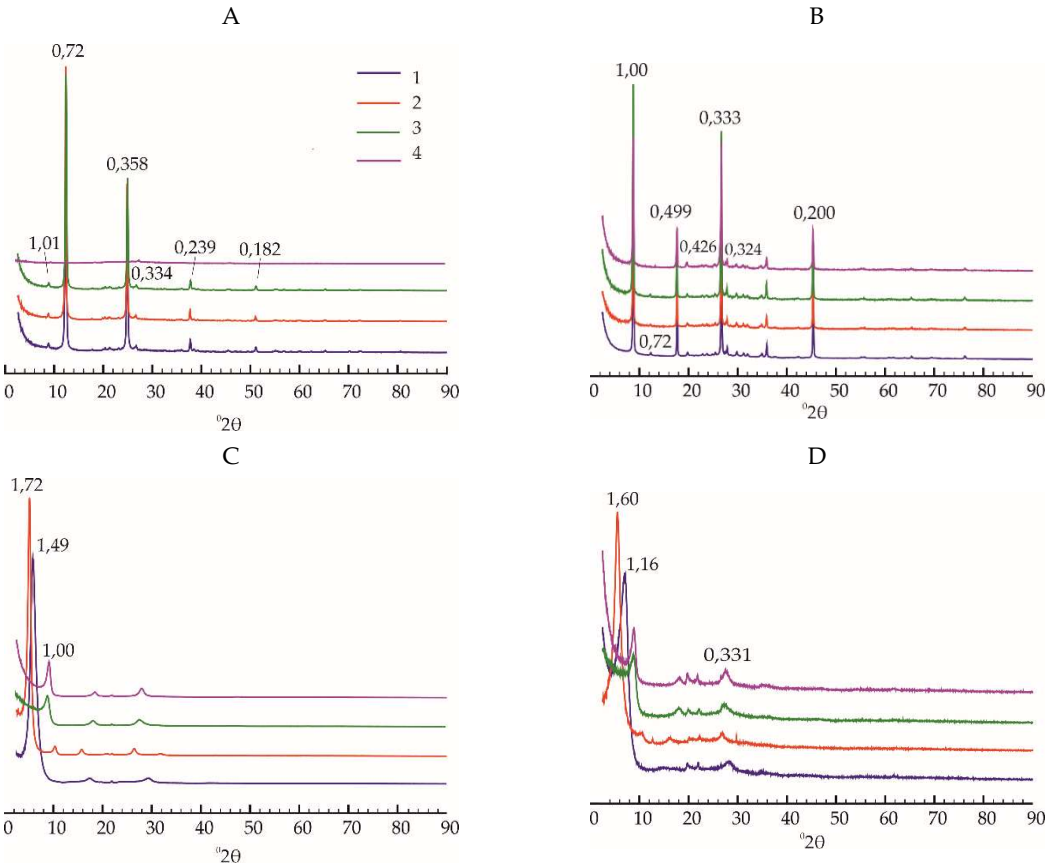

Figure 1. X-ray diffraction patterns for the clay fraction of kaolinite (A), muscovite (B), bentonite (C), and bentonite+HA (D) obtained for the samples in the air-dry state (1), saturated with ethylene glycol (2), calcined at temperature 350°C (3) and 550°C (4). The numbers on the curves are d/n in nm.

Thermal analysis of sorbents and sorbate. The DSC curve of kaolinite showed two endothermic effects: a weak one in the range of 35–100^{0}C that corresponds to the loss of hygroscopic moisture, and an intense one in the temperature range of 500–600^{0}C due to the dehydroxylation reaction (Figure 2A).

Preprints (www.preprints.org) | NOT PEER-REVIEWED | Posted: 28 August 2023 doi:10.20944/preprints202308.1813.v1

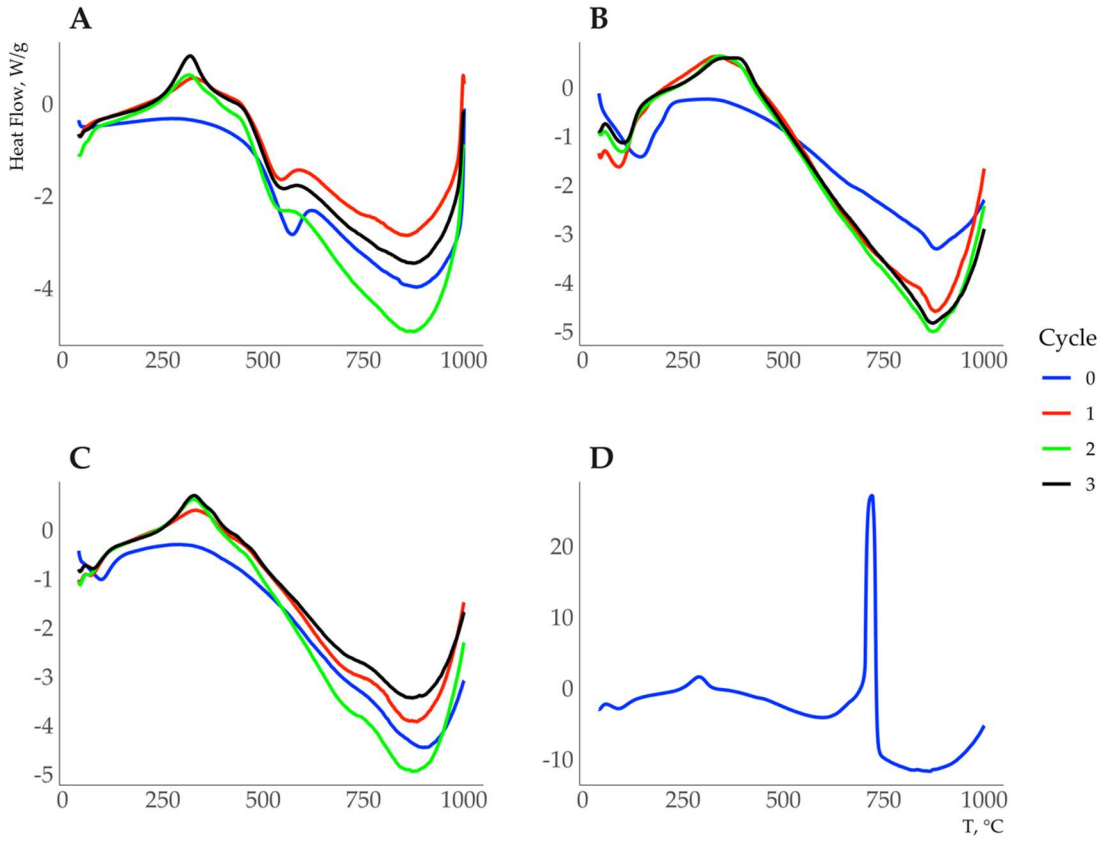

Figure 2. DSC curves for kaolinite (A), muscovite (B), bentonite (C), and HA (D). The blue, red, green, and black colors indicate the DSC curves of the sorbents before HA sorption and after the 1st, 2nd, and 3rd sorption cycles, respectively.

The DSC curves of muscovite showed two endothermic effects. The loss of a small amount of hygroscopic water under heating was accompanied by heat absorption within 80 to 140 ^{0}C. The second endothermic effect corresponded to a wide temperature range of 700 - 950 ^{0}C which destructs octahedral muscovite networks (Figure 2C). An intense two-peak low-temperature endothermic effect with maxima in the temperature ranges of 126-128 ^{0}C and 185-192 ^{0}C was well expressed on the DSC curve of bentonite. At high temperatures, this curve clearly showed the endothermic effect from 860 ^{0}C to 870 ^{0}C (Figure 2C). The DSC curve of the HA product showed a weak endothermic effect at 80 ^{0}C, an exothermic effect of medium intensity with a maximum at 290 ^{0}C, and a very intense exothermic effect with maximum intensity at a temperature of 740 ^{0}C (Figure 1D).

The endothermic effects of clay minerals and bentonite and the exothermic effects of HA were accompanied by a loss of sample mass (Figure 3).

Preprints (www.preprints.org) | NOT PEER-REVIEWED | Posted: 28 August 2023 doi:10.20944/preprints202308.1813.v1

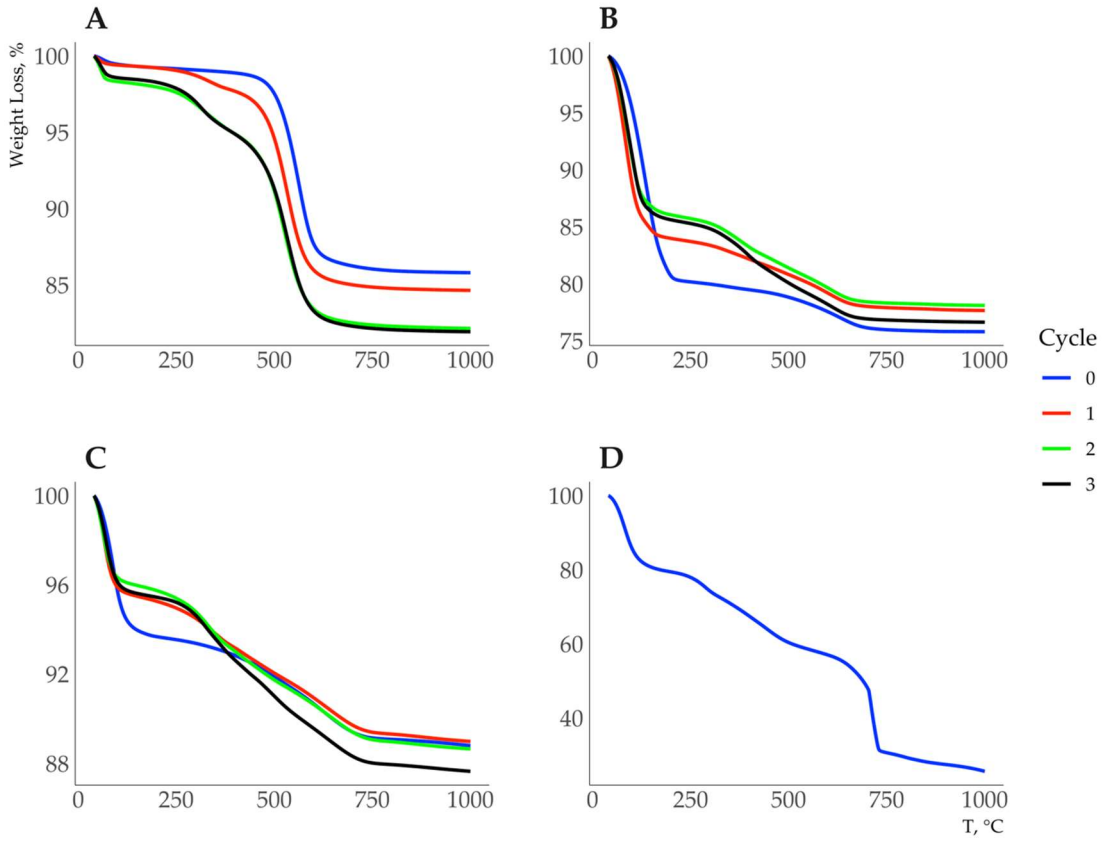

Figure 3. TG curves for kaolinite (A), muscovite (B), bentonite (C), and HA (D). The blue, red, green, and black colors indicate the DSC curves of the sorbents before HA sorption and after the 1st, 2nd, and 3rd sorption cycles, respectively.

Sorption of HA on kaolinite, muscovite and bentonite

Three cycles of HA sorption led to a change in the color of the minerals. The intensity of sorbent staining increased in the following order: muscovite < kaolinite < bentonite (Figure 4).

 doi:10.20944/preprints202308.1813.v1

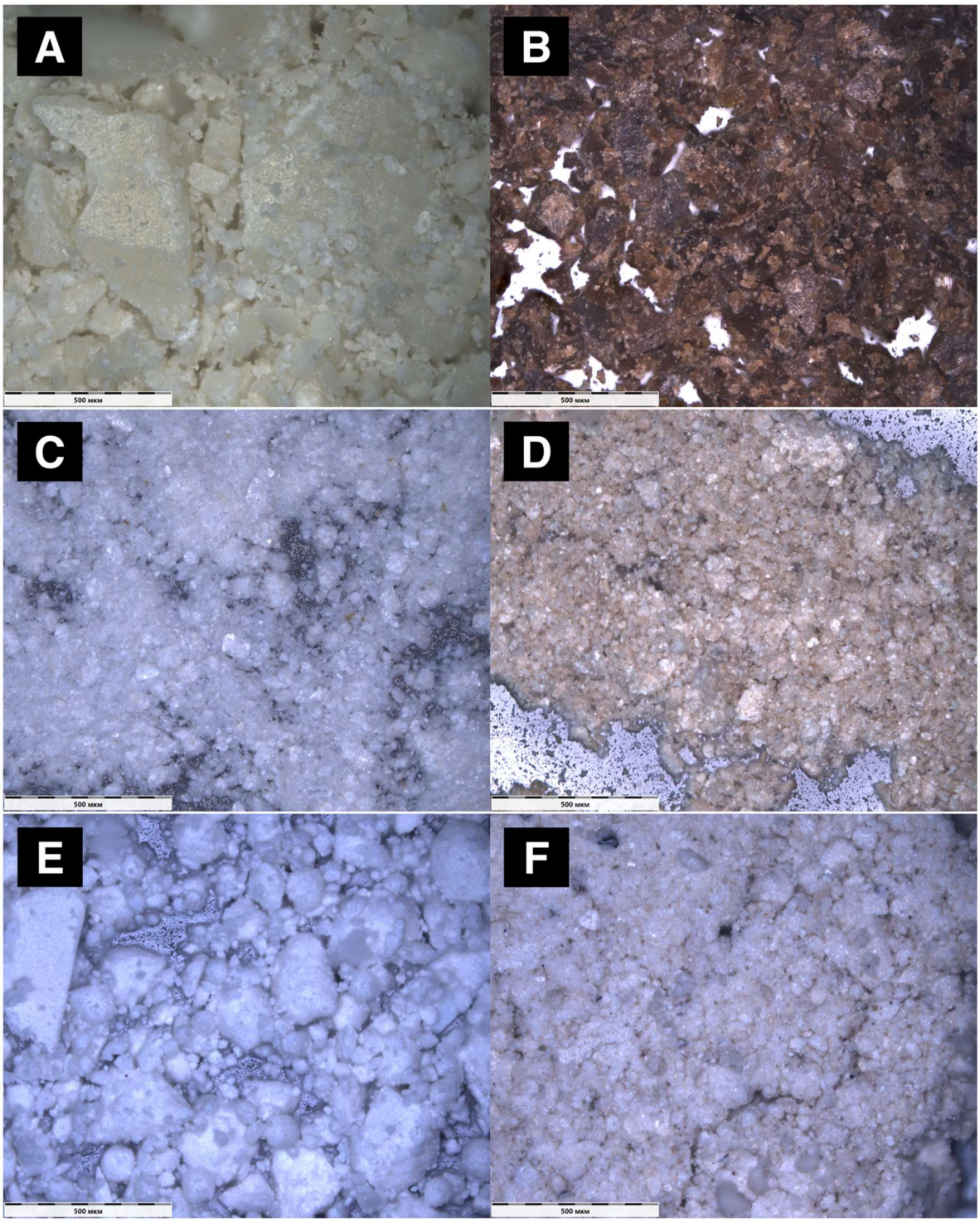

Figure 4. Photos of the mineral samples at 100x magnification (A - bentonite, B - bentonite + HA, C - kaolinite, D - kaolinite + HA, E - muscovite, F - muscovite + HA).

The SEM images showed no changes in the surface morphology of kaolinite and muscovite (Figure 5). Elongated and flow structures were found on the surface of bentonite after sorption of HA. The SEM X-ray probe allowed us to obtain their carbon content which was much higher compared to the original mineral without HA treatment. X-ray analysis of kaolinite and muscovite treated with HA did not reveal a significant increase in the carbon content on the surface of these minerals compared to the initial ones.

Preprints (www.preprints.org) | NOT PEER-REVIEWED | Posted: 28 August 2023 doi:10.20944/preprints202308.1813.v1

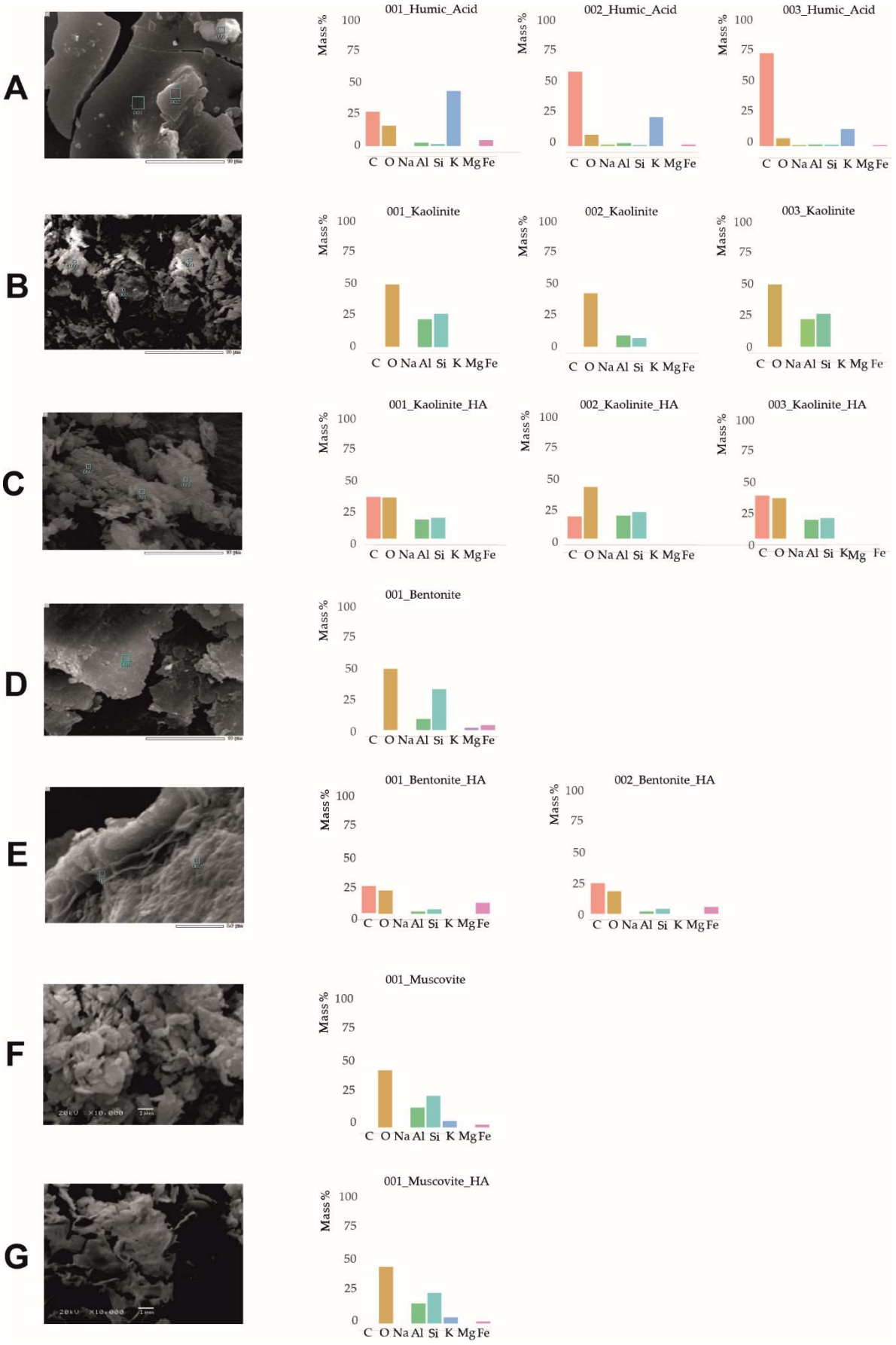

Figure 5. SEM images of the mineral samples at 10000x magnification (A - HA, B - kaolinite, C - kaolinite + HA, D - bentonite, E - bentonite + HA, F - muscovite, G - muscovite + HA.

Preprints (www.preprints.org) | NOT PEER-REVIEWED | Posted: 28 August 2023 doi:10.20944/preprints202308.1813.v1

The revealed regularities are consistent with the sorbed carbon content whose maximum amount calculated per unit mass (about 3%) was found in bentonite (Table 1).

Table 1. N and C content of HA in samples before and after HA sorption and surface characteristics of the sorbents.

Sample		Pore volume, cm^3/g	N, % *	C, % *	C/N *	S, m^2/g	C, g/m^2
Bentonite		0.084	0.18	0.09	1.3	88.7	1.02×10^{-5}
Kaolinite		0.107	0.12	0.09	2.1	18.7	4.81×10^{-5}
Muscovite		0.175	0.18	0.05	3.4	98.5	0.51×10^{-5}
HA		ND	0.91	40.35	44.2	ND	ND
Bentonite+HA	(1)	ND	0.17	3.18	18.7	ND	0.35×10^{-3}
	(2)	ND	0.17	3.01	17.7		
Kaolinite+HA	(1)	ND	0.08	2.11	26.4	ND	1.03×10^{-3}
	(2)	ND	0.06	1.75	29.1		
Muscovite+HA	(1)	ND	0.10	1.76	17.6	ND	0.18×10^{-3}
	(2)	ND	0.12	1.71	14.3		

* average of 3 analytical replicates. **Note:** ND, not determined.

The carbon content, expressed per unit mass of the sample after three sorption cycles, decreased in the series bentonite > kaolinite ≥ muscovite and correlated with neither surface area nor pore volume (Table 1). The sorbed HA was more enriched in N compared to the original HA. The organic matter sorbed on bentonite, muscovite, and kaolinite had the C/N ratio 2.4, 2.8, and 1.6 times lower compared to the initial HA, respectively (Table 1).

Sorption of humic acid occurred mainly due to hydrophobic components whose proportion decreased in the HA solution after sorption. Muscovite showed this decrease to a greater extent after HA sorption (Figure 6).

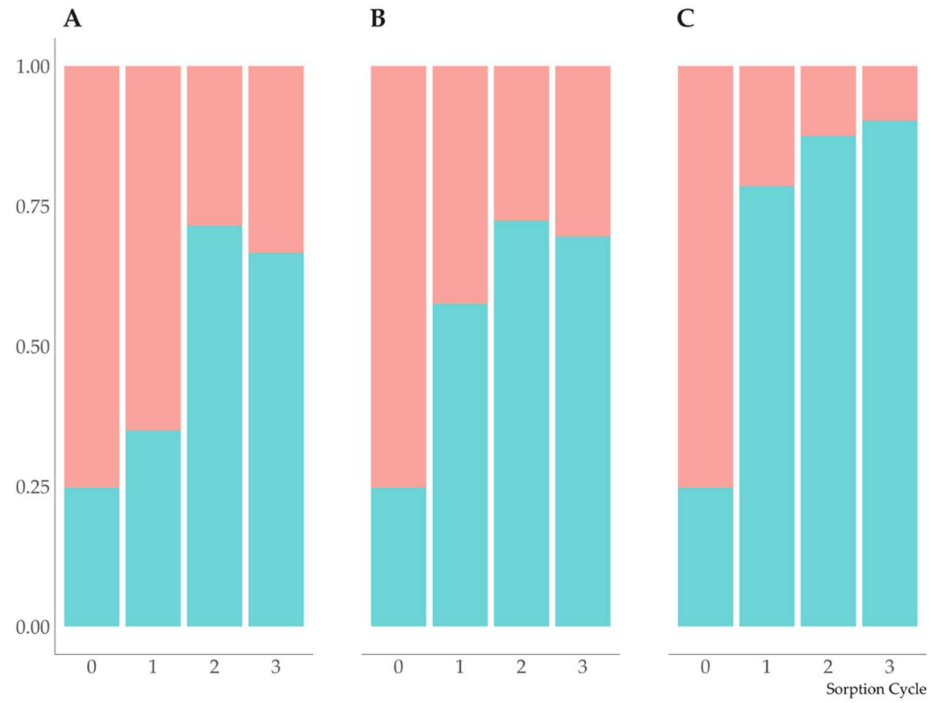

Figure 6. Ratio of hydrophilic (green) and hydrophobic (red) components in HA solution before and after sorption on minerals (A - kaolinite, B - bentonite, C - muscovite). 0 sorption cycle corresponds to the humic acid solution.

Preprints (www.preprints.org) | NOT PEER-REVIEWED | Posted: 28 August 2023 doi:10.20944/preprints202308.1813.v1

Thermal properties of minerals after sorption of HA on their surface. Two exothermic effects appeared on the DSC curves of minerals after the first and subsequent cycles of HA sorption in the range of 250–500 ^{0}C (Figure 2). Further in the text, these maxima are referred to as Exo1 and Exo2, respectively. The Exo1 and Exo2 maxima for kaolinite were diagnosed at 320 ^{0}C and in the range of 360-390 ^{0}C (Figure 2A), for bentonite - in the ranges of 330-350 ^{0}C and 370-390 °C (Figure 2C), and for muscovite at 330 ^{0}C and 360 ^{0}C, respectively (Figure 2B). The DSC curves of muscovite also revealed a weak exothermic effect in the range from 400 ^{0}C to 470 ^{0}C (Exo3). No intense exothermic effect was observed on the DSC curve of humic acid at 750 ^{0}C (Figure 2D) on the DSC curves of minerals after HA sorption. The DSC curves of minerals treated with humic acid exhibited a significant shift of the exothermic effects to the high temperature region relative to the initial exothermic effect of humic acid at 290°C (Figure 2).

The peak area ratio Exo1/Exo2 was maximum for muscovite and minimum for bentonite; the value of this ratio decreased from the first to the third sorption cycles (Figure 7).

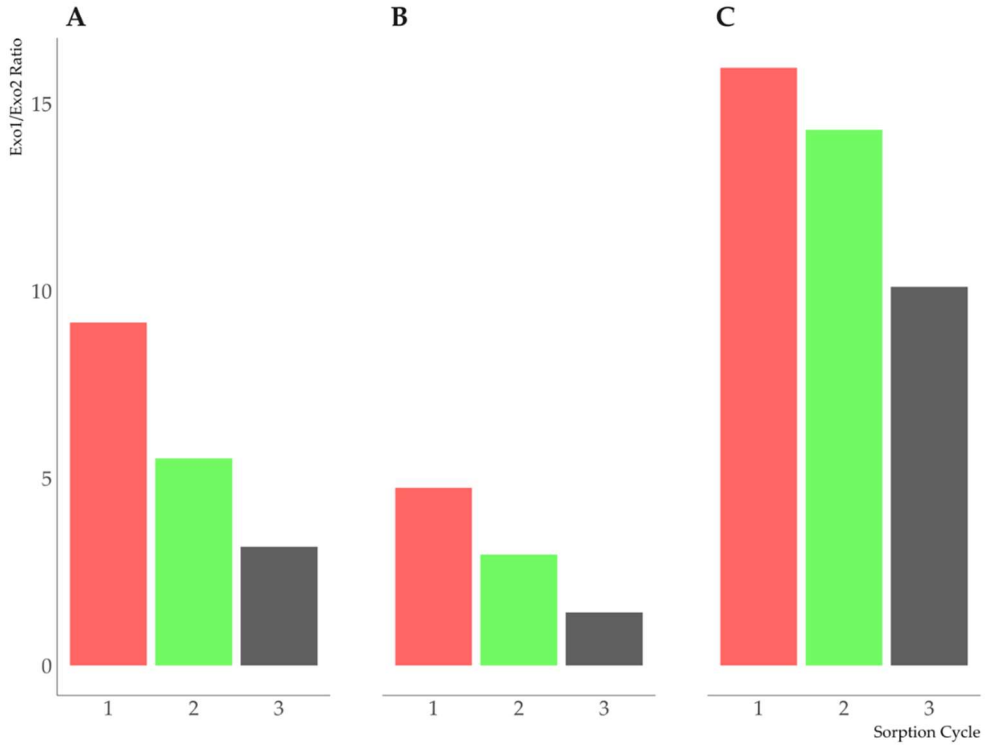

Figure 7. Exo1/Exo2 peak area ratio of kaolinite (A), bentonite (B) and muscovite (C). The colors correspond to the sorption cycles.

The DSC curves of kaolinite showed a shift of the endothermic effect of the mineral in the region of 500–550 ^{0}C to a lower temperature region after HA sorption (Figure 2A). For bentonite and muscovite no shift in the thermal effects of minerals associated with dehydroxylation was observed after sorption of HA.

In general, weight loss of the samples after HA sorption increased under heating within different temperatures (Figure 3, Table S1).

Dynamics of basal respiration. Basal respiration dynamics of humic acid, initial minerals, and minerals after HA sorption is shown in Figure 8. The rate of basal respiration for untreated bentonite and muscovite decreased sharply after 5 weeks of incubation, while the rate of basal respiration for kaolinite remained at a constant level except for 4 weeks which showed a sharp spike in CO_2 release. Basal respiration for HA-treated kaolinite and muscovite was maximal in the 1st week of incubation and sharply (by about 4 times) decreased during the incubation experiment. The basal respiration of

Preprints (www.preprints.org) | NOT PEER-REVIEWED | Posted: 28 August 2023 doi:10.20944/preprints202308.1813.v1

bentonite treated with a HA solution was almost 2 orders of magnitude less than that of other minerals and practically did not change during incubation (Figure 8).

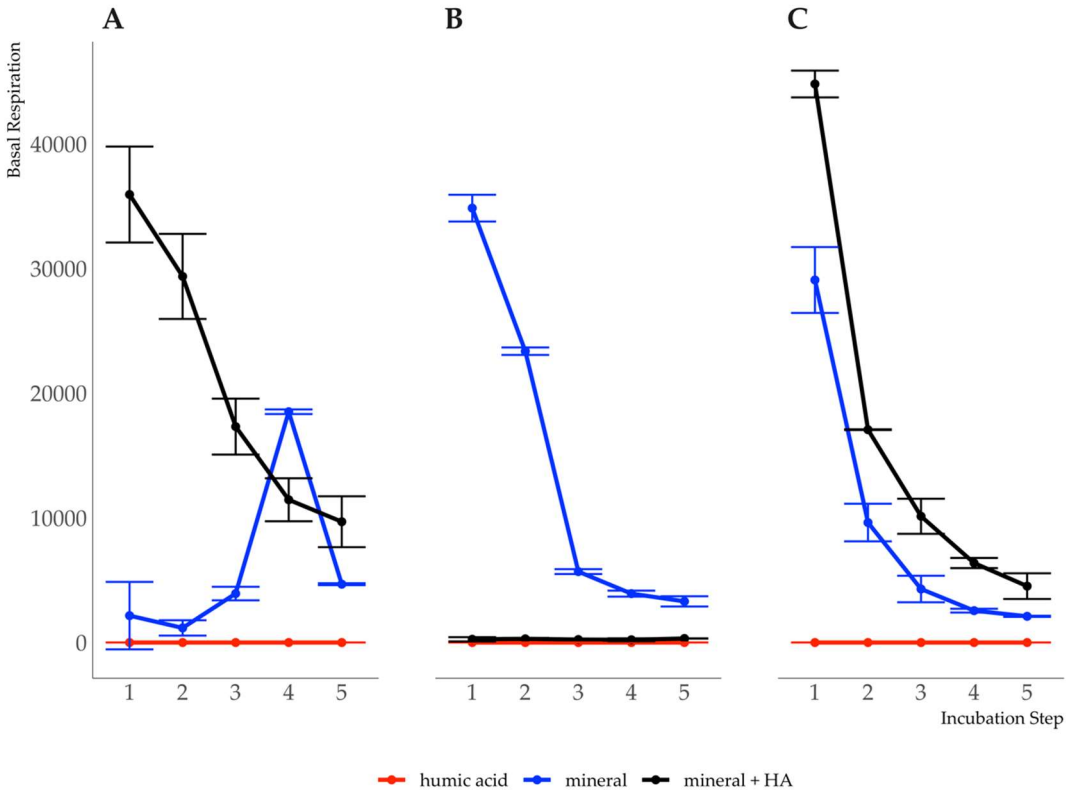

Figure 8. Basal respiration dynamics of humic acid in its pure form (red), as part of organo-mineral complexes (black) and raw minerals (blue). The y-axis is basal respiration, μg C-CO_2/g*h*(C, g), the abscissa is time intervals.

The intensity of HA basal respiration also showed little or no change during the incubation experiment.

4. Discussion

Sorption regularities of HA. The DSC curve of humic acid highlights an exothermic effect of medium intensity with a maximum at 290 ^{0}C, a weak exothermic effect accompanied by weight loss with a maximum of ≈ 470 ^{0}C, and a very intense exothermic effect with a maximum at a temperature of 740 ^{0}C (Figure 1C, Table S1). This can be explained by thermal destruction of various organic structures. According to the data obtained by the DSC, DTA, NMR, DRIFT-FTIR methods for HA whose composition is similar to the HA in our experiment, the exothermic effect at ≈300°C results from the destruction of carbohydrates and hydroxylated aliphatic structures. At ≈470°C, the destruction of polynuclear systems, long-chain hydrocarbons and nitrogen-containing substances occurs, and the products of polycondensation reaction, the most thermally stable aromatic structures, are destroyed at 700 ^{0}C [31,32]. The absence of a high-temperature exothermic effect at ≈ 700 ^{0}C on the DSC curves of kaolinite, bentonite, and muscovite after HA sorption at ≈ 700 ^{0}C (Figure 1 A-C) indicates that highly condensed thermally stable aromatic substances were not sorbed on minerals under the experimental conditions.

In terms of weight unit, the largest amount of HA was sorbed on bentonite (Table 1). The treatment of bentonite with a HA solution of pH 4.5 resulted in a partial replacement of Ca^{2+} by H^+ in the interlayers of montmorillonite and a decrease in the interplanar spacing of montmorillonite from 1.49 nm for Ca-montmorillonite to 1.25 nm for H(Ca)-montmorillonite (Figure 1 C, D). A decrease

 doi:10.20944/preprints202308.1813.v1

rather than an increase in the interplanar spacing of montmorillonite after HA sorption indicates that HA was sorbed on the mineral surface without intercalation into the interlayer space. The data obtained in experiments with soils also indicate that almost no HS intercalation occurs in the interlayers of montmorillonite [4,14].

Under the conditions of our experiment, humic acid was sorbed on all minerals mainly due to hydrophobic compounds (Figure 6). Therefore, the leading mechanism of HA sorption should be hydrophobic interactions which occur in areas of siloxane surfaces not affected by a constant negative charge of the mineral crystal lattice. The maximum amount of HAs was sorbed on kaolinite which is characterized by a low degree of isomorphic substitution in tetrahedra, hence a low layer charge per unit surface area. Bentonite, whose predominant mineral is montmorillonite with a low layer charge, sorbed less HAs per unit surface area than kaolinite. In terms of unit surface area, the least amount of HA was sorbed on muscovite which has a high negative charge in the tetrahedral network preventing hydrophobic interactions (Table 1).

The observed decrease in the proportion of hydrophobic components in the HA solution after the second and third cycles of sorption can be explained by two factors: zoning of the organic matter distribution near the mineral surface and heterogeneity of sorption centers on the surface of the original mineral and the mineral whose surface was modified by organic matter as a result of each subsequent sorption cycle (Figure 6). Unexpectedly, the hydrophobic fraction in the sorbed HA proved to be higher on muscovite which had less organic matter sorption due to the reasons described above. It is possible that the surface of muscovite had few hydrophobic sorption centers but they had a high selectivity. To explain this result, further research is required.

Sorption of HAs on clay minerals is accompanied by fractionation not only in amphiphilic properties, but also in chemical composition [3,5,10,33]. Kaolinite selectively sorbed the most nitrogen-depleted HA components, while bentonite and muscovite sorbed more nitrogen-containing components (Figure 6).

Obviously, hydrophilic components of HA are also sorbed on the surface of minerals. The pH of the zero charge point (pH_{PZC}) for bentonite clays is about 8 units [34–36], and the pKa of silanol and aluminol groups of montmorillonite vary from 6.7 to 8.2 and from 4.8 to 8.5, respectively [37,38]. The pH_{PZC} of the muscovite used in the experiment is 8.1 [39]. HA sorption was carried out at pH 4.5, which was lower than the pKa for the functional groups of the pH-dependent surfaces of kaolinite, muscovite, and montmorillonite. Thus, these functional groups were partially protonated and available for the sorption of deprotonated functional groups of HA whose pK_1 was 4.5. Amino groups at pH 4.5 were protonated and positively charged; therefore, they could also be fixed on the surface of minerals through electrostatic interaction. This mechanism is more probable in the case of HA sorption on muscovite, which has a high negative charge of the layer, and on montmorillonite. The above assumptions are confirmed by the low C/N values of organic matter adsorbed on muscovite and montmorillonite (Table 1). Bentonite, having a high cation exchange capacity and partially saturated Ca^{2+}, can retain HA by means of bridge bonds through the Ca^{2+} ion. The obtained data allow us to conclude that hydrophobic mechanism of HA sorption is mainly implemented on kaolinite, while the sorption of HA on muscovite is mostly determined by electrostatic interactions. Bentonite sorbs HA through both mechanisms.

Thermal stability of HA sorbed on minerals. Increased degradation temperature of HA and decreased peak area ratio Exo1/Exo2, decreasing in the series muscovite > kaolinite > bentonite (Figure 7), indicate an increase in more thermally stable organic matter on the surface of the solid phase compared to the initial HA. The asymmetry and bimodality of the exothermic effect of the sorbed HA destruction became most pronounced after the 3rd sorption cycle. This can be explained both by the sorption of HA components with different thermal stability and by the change in the thermal stability of HA due to multilayer sorption. According to the literature, during sorption on mineral surfaces HS molecules do not form a uniform layer, but are concentrated in limited areas (patches). If OM is increasing, it is sorbed mainly in these areas, forming layered structures [3,16,40]. In [13]proposed a conceptual model of multilayer HA sorption on kaolinite surface areas: saturation

 doi:10.20944/preprints202308.1813.v1

of the first layer of sorbed HA leads to the formation of a second layer on it, resulting in conformational changes in the first one, and so on.

According to our experiments, thermal stability of sorbed HA does not decrease with saturation, but, on the contrary, increases (the area of the Exo2 effect increases). Probably, the maximum sorption of organic matter was not achieved under the experimental conditions. Similar results were obtained by Feng et al. [20]. A decrease in weight loss in low-temperature regions and a corresponding increase in weight loss in high-temperature regions also indicate increased thermal stability of sorbed HA (Table S1). The results obtained can be explained by stronger fixation of HA on the surface of minerals due to the drying cycles of the experimental procedure or changed sorption properties of the mineral after forming an organomineral sorption complex [33].

After HA sorption, position of the endothermic effects of clay minerals dehydration shifts to lower temperatures and their position on the DSC curves almost coincide with that of the initial HA. HA appears to occupy a significant surface area of the mineral crystallites and, thus, determines the hygroscopic properties of the mineral.

The shift of the endothermic effect of kaolinite (dehydroxylation) to lower temperatures from 562°C in the initial kaolinite to 540–530°C after HA sorption can be explained by the weakening of bonds in the octahedral network and a decrease in its thermal stability. However, further studies are required to confirm this assumption.

Relationship between thermal stability of HA and resistance to microbial degradation. The intensity of basal respiration on the initial bentonite and muscovite (Figure 8) during the incubation experiment varied from 35000 to <5000 μg C-CO_2/g*h*(C, g). High vital activity of microorganisms at the first stages of the incubation experiment is explained by the availability of mineral nutrients suitable for utilization (potassium and calcium in muscovite, calcium in bentonite). Depletion of nutrient supply leads to a sharp decrease in the intensity of basal respiration at the last stages of the incubation experiment. For kaolinite, basal respiration did not exceed 5000 μg C-CO_2/g*h*(C, g) at all stages of the incubation experiment, except for a sharp increase at week 4 to 20000 μg C-CO_2/g*h*(C, g) (Figure 8). Minimum values of basal respiration for microorganisms on kaolinite are explained by a lack of nutrients. However, a sudden burst of microbial activity requires a separate study.

The basal respiration of microorganisms on minerals with adsorbed HA changed according to other regularities. For kaolinite and muscovite, the value of basal respiration proved to be higher compared to the corresponding initial minerals, which results from the utilization of sorbed organic matter. Decreased reserves of the substrate available for utilization led to a gradual decrease in the intensity of basal respiration. In muscovite, the decrease occurred faster than in kaolinite, which allows us to conclude that organic matter is more available on muscovite than on kaolinite.

In general, an inverse relationship was found between the intensity of basal respiration and increased degradation temperature of sorbed HA relative to free HA. This indicates decreased availability of sorbed HA for destruction by microorganisms as thermal stability and, presumably, the strength of bond with the mineral surface increase (Figure 9).

Preprints (www.preprints.org) | NOT PEER-REVIEWED | Posted: 28 August 2023 doi:10.20944/preprints202308.1813.v1

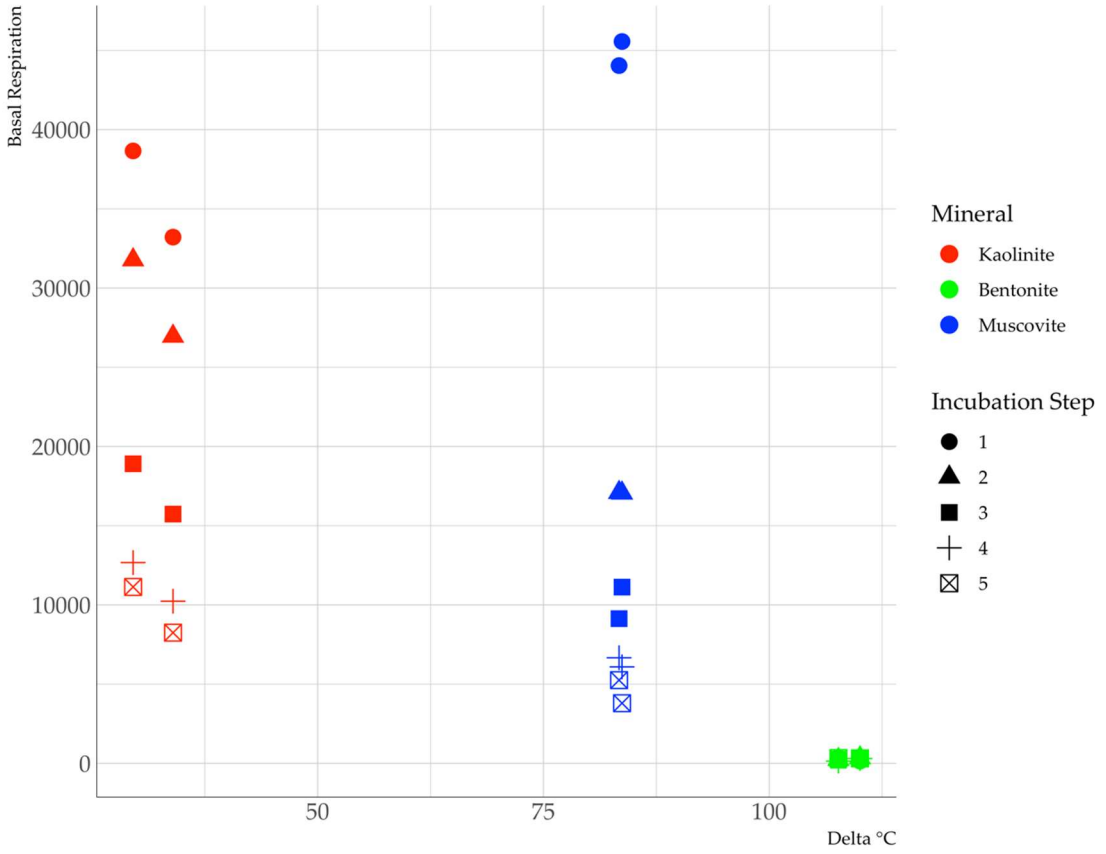

Figure 9. Dependence of the basal respiration on the increasing temperature of sorbed HA towards an increase in relation to non-sorbed HA.

The intensity of bentonite basal respiration with sorbed HA remained minimal throughout the entire incubation experiment (no more than 500 μg C-CO_2/g*h*(C, g)). The result obtained can be explained by low availability of organic matter for utilization by microorganisms. The bond between HA and montmorillonite via Ca^{2+} may be stronger than hydrophobic interactions on the surface of kaolinite and, to some extent, muscovite, and the electrostatic interactions are supposed to occur mostly on muscovite than on other minerals.

5. Conclusion

Under the experimental conditions, kaolinite sorbed more HA compared to bentonite and muscovite in terms of unit surface area. At pH 4.5, sorption was accompanied by HA fractionation in amphiphilicity and chemical composition. The C/N of sorbed HA was lower than that of free HA, which indicates selective sorption of nitrogen-containing compounds most characteristic of muscovite and bentonite. On the surface of all sorbents, HA was sorbed mainly due to hydrophobic components. It was established that during sorption no intercalation of HA into the interlayer spaces of montmorillonite occurred. Due to hydrophilic interactions sorption was performed mostly on muscovite and bentonite than on kaolinite.

Only a relatively thermolabile fraction was adsorbed on all minerals. Thermal stability of this fraction increased compared to the thermolabile HA fraction before the experiment. Stability of the sorbed HA components increased with each subsequent sorption cycle. Thermal stability and resistance to microbial oxidation of mineral-sorbed HA revealed the following relationship: the higher thermal stability, the less available is sorbed HA for utilization by microorganisms.

Acknowledgments: This work was supported by the Russian Foundation for Basic Research project No. 19-29-05028 mk. Determination of mineral composition of clay fraction was carried out on a MiniFlex 600 Rigaku

diffractometer purchased by Lomonosov Moscow State University within the Federal project "Development of advanced infrastructure for research and development in the Russian Federation" of the state project "Science" No. AM.6-pr. The study of organo-mineral complexes was performed using a Soptop CX40P standard light microscope purchased under the Development Program of Lomonosov Moscow State University.

References

1. Eusterhues, K.; Rumpel, C.; Kleber, M.; Kögel-Knabner, I. Stabilisation of Soil Organic Matter by Interactions with Minerals as Revealed by Mineral Dissolution and Oxidative Degradation. *Org Geochem* **2003**, *34*, 1591–1600, doi:10.1016/j.orggeochem.2003.08.007.
2. Saidy, A.R.; Smernik, R.J.; Baldock, J.A.; Kaiser, K.; Sanderman, J. Microbial Degradation of Organic Carbon Sorbed to Phyllosilicate Clays with and without Hydrous Iron Oxide Coating. *Eur J Soil Sci* **2015**, *66*, 83–94, doi:10.1111/ejss.12180.
3. Lützow, M. V.; Kögel-Knabner, I.; Ekschmitt, K.; Matzner, E.; Guggenberger, G.; Marschner, B.; Flessa, H. Stabilization of Organic Matter in Temperate Soils: Mechanisms and Their Relevance under Different Soil Conditions - A Review. *Eur J Soil Sci* 2006, *57*, 426–445.
4. Chen, H.; Koopal, L.K.; Xiong, J.; Avena, M.; Tan, W. Mechanisms of Soil Humic Acid Adsorption onto Montmorillonite and Kaolinite. *J Colloid Interface Sci* **2017**, *504*, 457–467, doi:10.1016/j.jcis.2017.05.078.
5. El-sayed, M.E.A.; Khalaf, M.M.R.; Gibson, D.; Rice, J.A. Assessment of Clay Mineral Selectivity for Adsorption of Aliphatic/Aromatic Humic Acid Fraction. *Chem Geol* **2019**, *511*, 21–27, doi:10.1016/j.chemgeo.2019.02.034.
6. Chen, H.; Li, Q.; Wang, M.; Ji, D.; Tan, W. XPS and Two-Dimensional FTIR Correlation Analysis on the Binding Characteristics of Humic Acid onto Kaolinite Surface. *Science of the Total Environment* **2020**, *724*, doi:10.1016/j.scitotenv.2020.138154.
7. Bougdah, N.; Messikh, N.; Bousba, S.; Magri, P.; Djazi, F.; Zaghdoudi, R. Adsorption of Humic Acid from Aqueous Solution on Different Modified Bentonites. *Chem Eng Trans* **2017**, *60*, 223–228, doi:10.3303/CET1760038.
8. Al-Essa, K. Adsorption of Humic Acid onto Jordanian Kaolinite Clay: Effects of Humic Acid Concentration, PH, and Temperature. *Science Journal of Chemistry* **2018**, *6*, 1, doi:10.11648/j.sjc.20180601.11.
9. Gouré-Doubi, H.; Martias, C.; Smith, A.; Villandier, N.; Sol, V.; Gloaguen, V.; Feuillade, G. Adsorption of Fulvic and Humic like Acids on Surfaces of Clays: Relation with SUVA Index and Acidity. *Appl Clay Sci* **2018**, *154*, 83–90, doi:10.1016/j.clay.2017.12.036.
10. Zhang, L.; Luo, L.; Zhang, S. Integrated Investigations on the Adsorption Mechanisms of Fulvic and Humic Acids on Three Clay Minerals. *Colloids Surf A Physicochem Eng Asp* **2012**, *406*, 84–90, doi:10.1016/j.colsurfa.2012.05.003.
11. Elfarissi, F.; Pefferkorn, E. *Kaolinite/Humic Acid Interaction in the Presence of Aluminium Ion*; 2000; Vol. 168;.
12. Kloster, N.; Avena, M. Interaction of Humic Acids with Soil Minerals: Adsorption and Surface Aggregation Induced by Ca2+. In Proceedings of the Environmental Chemistry; CSIRO, 2015; Vol. 12, pp. 731–738.
13. Zhu, X.; He, J.; Su, S.; Zhang, X.; Wang, F. Concept Model of the Formation Process of Humic Acid-Kaolin Complexes Deduced by Trichloroethylene Sorption Experiments and Various Characterizations. *Chemosphere* **2016**, *151*, 116–123, doi:10.1016/j.chemosphere.2016.02.068.
14. Chotzen, R.A.; Polubesova, T.; Chefetz, B.; Mishael, Y.G. Adsorption of Soil-Derived Humic Acid by Seven Clay Minerals: A Systematic Study. *Clays Clay Miner* **2016**, *64*, 628–638, doi:10.1346/CCMN.2016.064027.
15. Lehmann, J.; Kleber, M. The Contentious Nature of Soil Organic Matter. *Nature* 2015, *528*, 60–68.
16. Kleber, M.; Sollins, P.; Sutton, R. A Conceptual Model of Organo-Mineral Interactions in Soils: Self-Assembly of Organic Molecular Fragments into Zonal Structures on Mineral Surfaces. *Biogeochemistry* **2007**, *85*, 9–24, doi:10.1007/s10533-007-9103-5.
17. Barré, P.; Fernandez-Ugalde, O.; Virto, I.; Velde, B.; Chenu, C. Impact of Phyllosilicate Mineralogy on Organic Carbon Stabilization in Soils: Incomplete Knowledge and Exciting Prospects. *Geoderma* 2014, *235–236*, 382–395.
18. Dell'abate, M.T.; Benedetti, A.; Brookes, P.C. *Hyphenated Techniques of Thermal Analysis for Characterisation of Soil Humic Substances 1)*;
19. Mao, J.; Fang, X.; Schmidt-Rohr, K.; Carmo, A.M.; Hundal, L.S.; Thompson, M.L. Molecular-Scale Heterogeneity of Humic Acid in Particle-Size Fractions of Two Iowa Soils. *Geoderma* **2007**, *140*, 17–29, doi:10.1016/j.geoderma.2007.03.014.
20. Feng, W.; Plante, A.F.; Aufdenkampe, A.K.; Six, J. Soil Organic Matter Stability in Organo-Mineral Complexes as a Function of Increasing C Loading. *Soil Biol Biochem* **2014**, *69*, 398–405, doi:10.1016/j.soilbio.2013.11.024.
21. Gregorich, E.G.; Gillespie, A.W.; Beare, M.H.; Curtin, D.; Sanei, H.; Yanni, S.F. Evaluating Biodegradability of Soil Organic Matter by Its Thermal Stability and Chemical Composition. *Soil Biol Biochem* **2015**, *91*, 182–191, doi:10.1016/j.soilbio.2015.08.032.

22. Plante, A.F.; Fernández, J.M.; Leifeld, J. Application of Thermal Analysis Techniques in Soil Science. *Geoderma* 2009, *153*, 1–10.
23. Fernández, J.M.; Peltre, C.; Craine, J.M.; Plante, A.F. Improved Characterization of Soil Organic Matter by Thermal Analysis Using CO2/H2O Evolved Gas Analysis. *Environ Sci Technol* **2012**, *46*, 8921–8927, doi:10.1021/es301375d.
24. Peltre, C.; Fernández, J.M.; Craine, J.M.; Plante, A.F. Relationships between Biological and Thermal Indices of Soil Organic Matter Stability Differ with Soil Organic Carbon Level. *Soil Science Society of America Journal* **2013**, *77*, 2020–2028, doi:10.2136/sssaj2013.02.0081.
25. Plante, A.F.; Fernández, J.M.; Haddix, M.L.; Steinweg, J.M.; Conant, R.T. Biological, Chemical and Thermal Indices of Soil Organic Matter Stability in Four Grassland Soils. *Soil Biol Biochem* **2011**, *43*, 1051–1058, doi:10.1016/j.soilbio.2011.01.024.
26. Karavanova, E.I. Dissolved Organic Matter: Fractional Composition and Sorbability by the Soil Solid Phase (Review of Literature). *Eurasian Soil Science* **2013**, *46*, 833–844, doi:10.1134/S1064229313080048.
27. Chechetko, E.S.; Tolpeshta, I.I.; Zavgorodnyaya, Yu.A. Application of Dodecyltrimethylammonium-Modified Bentonite for Water Purification from Oil and Water-Soluble Oil Components. *Moscow University Soil Science Bulletin* **2017**, *72*, 119–124, doi:10.3103/s0147687417030036.
28. Semenov, A.A.; Demin, V.V.; Biryukov, M.V.; Zavgorodnyaya, Yu.A. Lokalizaciya Bioprotektornogo Dejstviya Guminovyh Veshchestv v Pochvah. *Estestvennye tekhnicheskie nauki* **2008**, *4*, 84–93.
29. Barreto, M.S.C.; Ramlogan, M.; Oliveira, D.M.S.; Verburg, E.E.J.; Elzinga, E.J.; Rouff, A.A.; Jemo, M.; Alleoni, L.R.F. Thermal Stability of Soil Organic Carbon after Long-Term Manure Application across Land Uses and Tillage Systems in an Oxisol. *Catena (Amst)* **2021**, *200*, doi:10.1016/j.catena.2021.105164.
30. Wickham H *Ggplot2: Elegant Graphics for Data Analysis*; 3rd ed.; Springer-Verlag New York, 2016; ISBN 978-3-319-24277-4.
31. Francioso, O.; Montecchio, D. *Diffuse Reflectance Fourier Transform Spectroscopy and Thermal Analysis Applied to Humic Substances Espectroscopía Por Transformada de Fourier de Reflectancia Difusa y Análisis Térmico Aplicados a Substancias Húmicas*; 2007; Vol. 40;.
32. Francioso, O.; Montecchio, D.; Gioacchini, P.; Ciavatta, C. Thermal Analysis (TG-DTA) and Isotopic Characterization (13C-15N) of Humic Acids from Different Origins. *Applied Geochemistry* **2005**, *20*, 537–544, doi:10.1016/j.apgeochem.2004.10.003.
33. Ghosh, S.; Wang, Z.Y.; Kang, S.; Bhowmik, P.C.; Xing, B.S. Sorption and Fractionation of a Peat Derived Humic Acid by Kaolinite, Montmorillonite, and Goethite Project Supported by the Federal Hatch Program, USA (No. MAS 8532); the Cheung Kong Scholar Program, Ministry of Education of China; and the CSREES, USDA National Research Initiative Competitive Grants Program, USA (No. 2005-35107-15278). *Pedosphere* **2009**, *19*, 21–30, doi:10.1016/S1002-0160(08)60080-6.
34. Dimirkou, A.; Ioannou, A.; Doula, M. Preparation, Characterization and Sorption Properties for Phosphates of Hematite, Bentonite and Bentonite-Hematite Systems. *Adv Colloid Interface Sci* 2002, *97*, 37–61.
35. Kim Dong-Su Measurment of Point of Zero Charge of Bentonite by Solubilization Technique and Its Dependence of Surface Potential on PH. *Environmental Engineering Research* **2003**, *8*, 222–227.
36. Hernández-Hernández, K.A.; Solache-Ríos, M.; Díaz-Nava, M.C. Removal of Brilliant Blue FCF from Aqueous Solutions Using an Unmodified and Iron-Modified Bentonite and the Thermodynamic Parameters of the Process. *Water Air Soil Pollut* **2013**, *224*, doi:10.1007/s11270-013-1562-9.
37. Zachara, J.M.; Smith, S.C. *Edge Complexation Reactions of Cadmium on Specimen and Soil-Derived Smectite*;
38. Liu, X.; Lu, X.; Sprik, M.; Cheng, J.; Meijer, E.J.; Wang, R. Acidity of Edge Surface Sites of Montmorillonite and Kaolinite. *Geochim Cosmochim Acta* **2013**, *117*, 180–190, doi:10.1016/j.gca.2013.04.008.
39. Kolchanova, K.; Tolpeshta, I.; Izosimova, Y. Adsorption of Fulvic Acid and Water Extractable Soil Organic Matter on Kaolinite and Muscovite. *Agronomy* **2021**, *11*, doi:10.3390/agronomy11122420.
40. Kaiser, K.; Guggenberger, G. Mineral Surfaces and Soil Organic Matter. *Eur J Soil Sci* **2003**, *54*, 219–236, doi:10.1046/j.1365-2389.2003.00544.x.